Advances in Concrete Construction, *Vol. 8, No. 4 (2019) 295-304*
DOI: https://doi.org/10.12989/acc.2019.8.4.295

Comparison of displacement capacity of reinforced concrete columns with seismic codes

Sinan Cansız*[1], Cem Aydemir[2a] and Güray Arslan[3b]

[1]*Department of Construction Technology, Istanbul Aydın University, Istanbul, Turkey*
[2]*Department of Civil Engineering, Istanbul Aydın University, Istanbul, Turkey*
[3]*Department of Civil Engineering, Yildiz Technical University, Istanbul, Turkey*

(*Received April 18, 2018, Revised September 25, 2019, Accepted October 11, 2019*)

Abstract. The lateral displacement or drift may be the cause of the damage in the reinforced concrete (RC) columns under the seismic load. In many regulations, lateral displacement was limited according to the properties of columns. The design displacement limits may be represented indirectly through the material strain limits and the mechanical properties of columns. EUROCODE-8 and FEMA356 calculate displacement limits by taking into account the mechanical properties of columns. However, Turkey Building Earthquake Code (TBEC) determine displacement limits by taking into account the material strain limits. The aim of this study is to assess the seismic design codes for RC columns through an experimental study. The estimates of seismic design codes have been compared with the experimental results. It is observed that the lateral displacement capacities of columns estimated according to some seismic codes are not in agreement with the experimental results. Also, it is observed that TBEC is conservative in the context of the performance indicator of RC columns, compared to EUROCODE-8 and FEMA356. Moreover, in this study, plastic hinge length and effective stiffness of test elements were investigated.

Keywords: drift capacity; reinforced concrete; columns; plastic hinge length; effective stiffness

1. Introduction

Displacement capacity of reinforced concrete (RC) columns has been the subject of significant research activity among the earthquake engineering community for over three decades (Au and Bai 2006, Cao *et al*. 2014). In general, performance-based design is a method that expresses structural performance in terms of material strain, drift or displacement. The curvature capacity of the section and the drift capacity of the element are important parameters in evaluating the performance of the columns. Priestley *et al*. (1998) resulted in the recognition that the basis of the force-based seismic design approach depends largely on inaccurate assumptions. Moreover, Priestley *et al*. (1998) proposed expressions for curvatures and drifts based on material strains. Brachmann *et al*. (2004) defined a direct relationship between the limiting drift ratio and the corresponding material and structural properties of RC columns.

Panagiotakos and Fardis (2001) provided formulations for chord rotation capacity at yielding and “ultimate” (at 20% strength drop), the latter through an empirical and a semi-empirical (i.e., based on the plastic hinge length) approach based on a large database of flexure-controlled experimental tests for RC elements. The recommendations of Fardis *et al*. (2001) were adopted by EUROCODE-8 and the limit value was accepted as the Collapse Limit State. Elwood and Moehle (2005) proposed empirical formulations providing the expected drift at “collapse” (20% strength decrease) and at “axial failure” (loss of vertical load carrying capacity) of RC columns failing in shear following flexural yielding. The predicted drift at the initiation of longitudinal bar buckling, which may limit the calculated deformation capacity at collapse limit for flexure-controlled columns, was evaluated through the empirical formulation defined by Berry and Eberhard (2005). Pujol *et al*. (2006) developed a procedure to estimate the limiting drift ratio at which no significant loss of shear capacity occurs in terms of the average shear stresses, the amount of transverse reinforcement and the shear span-to-depth ratio. The Seismic Assessment of Existing Buildings (NZSEE, 2017) adopted a procedure for the estimation of the deformation capacity at Ultimate Limit State (ULS) based on plastic hinge length approach, referring to Priestley *et al*. (2007). While many researchers (Bhosale *et al*. 2017, Behnam and Sjojaei 2018) examine seismic analysis on structure basis, others investigate seismic analysis on element basis. Several studies have been conducted for prediction of the ultimate deformation capacity (Nishitani *et al*. 2014, Bae *et al*. 2005, Ascheim 2002, Lehmann and Moehle 2000, Mander *et al*. 1988, Park and Paulay 1975, Priestley and Park 1987, Cao and Ronagh 2013, Zhou *et al*. 2019, Gharehbaghi *et al*. 2016, Kang and Lee 2016, Arslan *et al*. 2013, Sezen 2008, Shojaei *et al*. 2017, Puranam *et al*. 2018, Abdullah and Wallace 2019, Al

*Corresponding author, Ph.D. Student
E-mail: sinancansiz@aydin.edu.tr
[a]Associate Professor
E-mail: cemaydemir@aydin.edu.tr
[b]Professor
E-mail: aguray@yildiz.edu.tr

http://www.techno-press.org/?journal=acc&subpage=7
ISSN: 2287-5301 (Print), 2287-531X (Online)

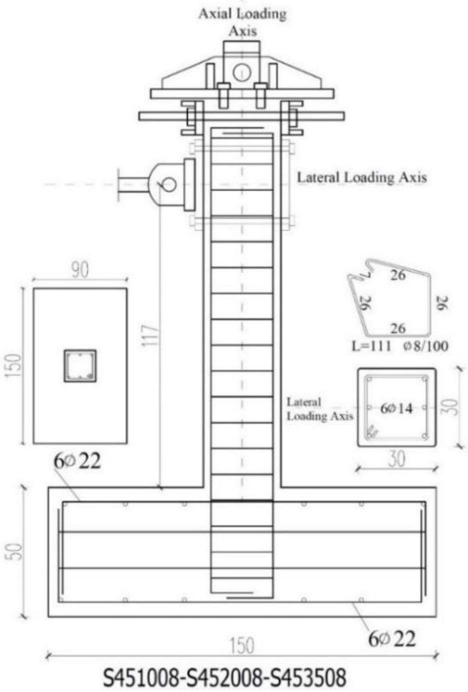

Fig. 1 Column geometry and reinforcement

Table 1 Specimen properties

Parameter		Specimens		
		S451008	S452008	S453508
Axial Load	N (kN)	292.5	595	1000
	$N/(A_c \times f'_c)$	0.10	0.20	0.35
Geometric	$b/h/d$ (cm/cm/cm)	30/30/26	30/30/26	30/30/26
	(a/d) (cm/cm)	117/26=4.5	117/26=4.5	117/26=4.5
Material	f'_c (MPa)	32.5	33.0	32.0
	$f_y/f_{su}/f_{yw}$ (MPa)	484/637 /690	484/637 /690	484/637 /690
	$\varepsilon_{sh}/\varepsilon_{su}$	0.009/0.14	0.009/0.14	0.009/0.14
Reinforcement	Flexural reinforcement (Ratio, ρ_l)	6ϕ14 (0.0103)	6ϕ14 (0.0103)	6ϕ14 (0.0103)
	Shear reinforcement (Volumetric ratio, ρ_h)	ϕ8/10 (0.008)	ϕ8/10 (0.008)	ϕ8/10 (0.008)

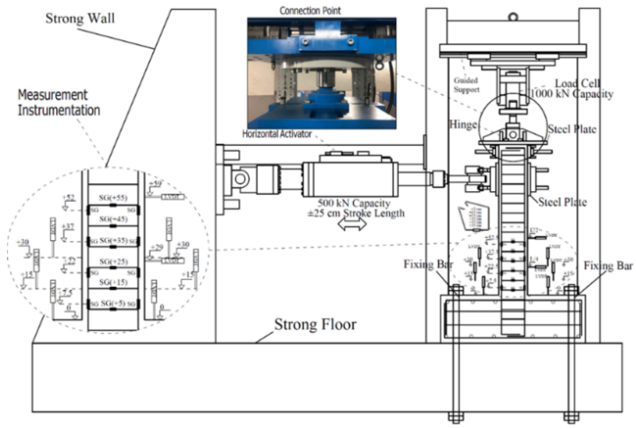

Fig. 2 Test configuration and instrumentation

Abadi *et al*. 2019, Wibowo *et al*. 2014).

The aim of this study is to examine the shear and bending behavior of RC columns under cyclic loading similar to the earthquake loads combined with variable axial load level. The experimental results are compared with the estimates of seismic design codes. It is observed that the estimates of some codes are not in agreement with the experimental results.

2. Experimental program

Within the scope of this study, three column samples were produced and tested in Civil Engineering Construction Laboratory at Istanbul Aydin University.

2.1 Specimen

Three columns were designed and tested quasi-statically. The columns had cross-sections of 300 mm by 300 mm, and were approximately 1170 mm high. All specimens had the same reinforcing bars. The drawings of reinforcement, the geometric properties and the material properties of test specimens are given in Fig. 1 and Table 1. Both alphabetic and numeric characters were used for labeling test specimens. The first two digits in the labels show the shear span-to-effective depth ratio (a/d), the next two digits show the axial load level and the last two digits show the volumetric lateral reinforcement ratio. For example, for S451008, the *a/d* is 4.5, the axial load level is 0.1 and the lateral reinforcement volume is 0.008.

Lateral load was applied by a displacement controlled 1000-kN-capacity horizontal hydraulic actuator. S451008-S452008-S453508 specimens were subjected to constant compressive axial loads of 292.5 kN, 595 kN and 1000 kN, respectively. The average measured concrete cylinder strength (f_c) was about 32 MPa on the day of tests. Six 14-mm diameter longitudinal bars were used for a longitudinal reinforcement ratio of 1.0%. The average yield strength (f_y) and the ultimate strength of longitudinal bars (f_{su}) were 484 MPa and 637 MPa, respectively. The measured yield strength of 8-mm-diameter deformed transverse reinforcement (f_{yw}) were 690 MPa.

2.2 Test setup

The test specimen elevation, typical column cross-section, and test setup are shown in Fig. 2. Strain gages were attached on the longitudinal and transverse reinforcement to monitor the strain variations along the height of the columns. For testing a column, the bottom end was fixed to the strong floor as a cantilever. The top displacement was provided by a horizontal activator. A guided support was used for the horizontal displacement of the test setup. The column was connected to the test setup by a hinge which was free to rotate so that the direction of the axial load did not change.

2.3 Loading histories

A similar procedure was used for each test specimen.

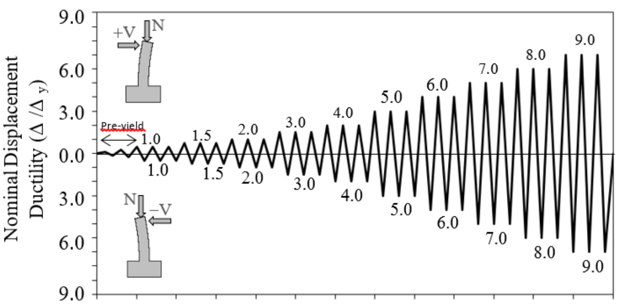

Fig. 3 Displacement ductility history for specimens

Table 2 Comparison of flexural and shear capacities of specimens

Specimens	M_n(1) (kN.m)	V_n(2) (kN)	V_{flex}(3) (kN)	V_{max}(4) (kN)	M_{max}(5) (kN.m)	Failure Mode(6)
S451008	87.4	260.3	74.7	80.3	104.0	F
S452008	115.8	260.9	98.9	99.9	128.5	F
S453508	132.9	259.7	113.5	103.8	135.6	F

(1) Nominal flexural strength calculated based on ACI 318,
(2) Nominal shear strength (V_c+V_s) calculated based on ACI 318,
(3) Nominal flexural moment capacity/L_{column} based on ACI 318
(4) Maximum shear demand,
(5) Maximum flexural demand,
(6) *F*: Flexural failure.

The axial load was applied at the beginning of a test and was maintained constant during testing. The constant axial load values of 292.5 kN, 595 kN and 1000 kN were applied to S451008, S452008 and S453508 respectively. The target lateral displacement history is shown in Fig. 3. All specimens were subjected to the same lateral displacement history. For each specimen, one full cycle of loading was performed in the pre-yield stage. The pre-yield stage consisted of 0.5Δ_y and 0.25Δ_y. Then the test specimen was subjected to cyclic loading with increasing amplitudes after every three cycles up to failure. In addition, the standard loading histories are obtained from the studies of Kunnath *et al*. (1997), Elwood and Moehle (2005). The data were collected electronically as approximately 10 data per second. Also, damage patterns, concrete cracking, initial yield, spalling, reinforcement buckling and fracture were recorded.

3. Test results

All specimens were designed to fail due to concrete crushing in the plastic hinges after flexural yielding. The shear and bending capacities of the test specimens are presented in Table 2.

The moment-axial load interaction diagram of all specimens is presented in Fig. 4. All specimens failed in flexure.

3.1 Type of damage

S451008

The specimen S451008 with an *a/d* of 4.5 and an axial load ratio (*N/Acfc*) of 10% was able to sustain a maximum drift of 4.7% (55 mm) before gravity load collapse with plastic hinge formation at the base of the column as shown in Fig. 5(d). At a drift ratio of 1% (11 mm deflection), first cracks were observed above the footing surface and the initial yield value was measured by strain-gages (Fig. 5(b)). As the displacement reached a drift ratio of 2.8% (33 mm), slight crushing was observed due to spalling of the cover concrete within a height of 150 mm above the footing (Fig. 5(c)). The total length of the crushed concrete was about 200 mm near the footing surface, implying the formation of a plastic hinge near the footing. No damage was observed above a height of 900 mm. From the ductility standpoint, assuming the first yield of the longitudinal steel as the yield point, corresponding to a drift ratio of 0.94%, the column achieved a ductility of slightly more than 5 before the flexural failure. The damage at collapse in the vicinity of the support is shown in Fig. 6.

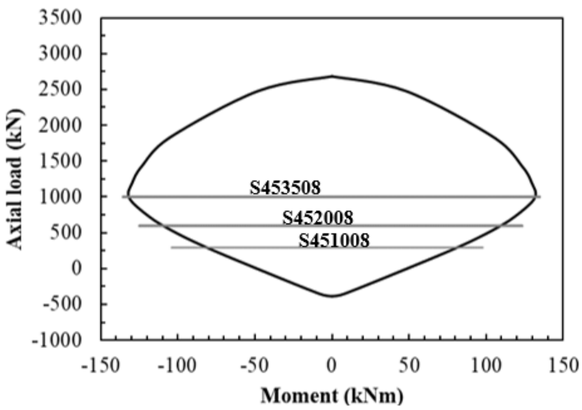

Fig. 4 Moment-axial load interaction for specimens

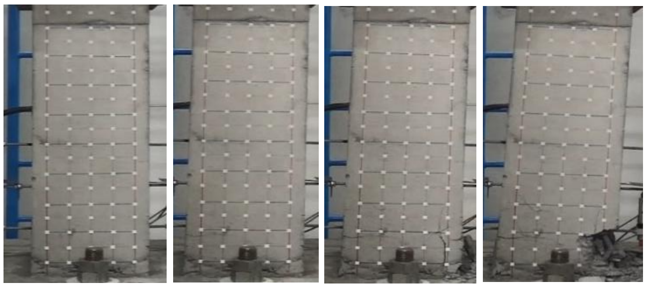

(a) (b) (c) (d)

Fig. 5 Different drift ratio belong to S451008, (a) % 0 None loading, (b) %1 yield stage (c) %2.8 spalling cover concrete (d) %4.7 flexural failure mode

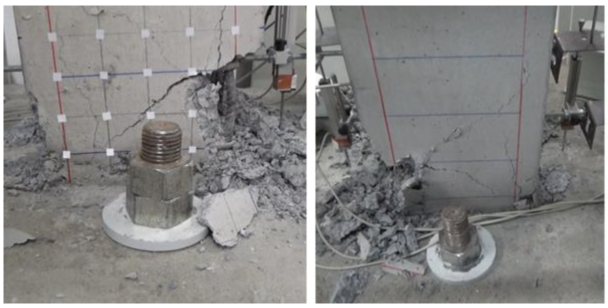

Fig. 6 Various damage photos for S451008

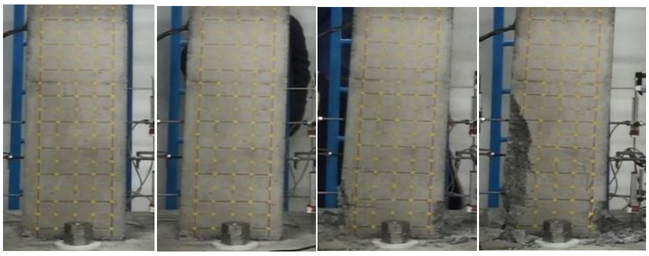

(a) (b) (c) (d)

Fig. 7 Different drift ratio belong to S452008, (a) % 0 None loading, (b) %0.6 yield stage (c) %2.7 spalling cover concrete (d) %3.4 flexural failure mode

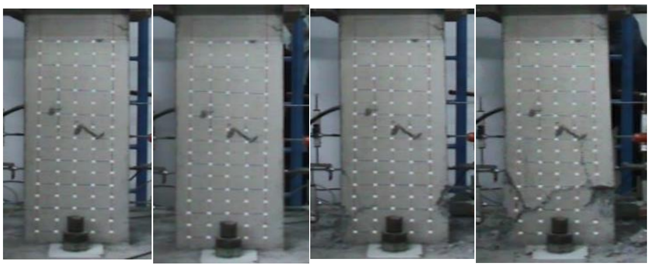

(a) (b) (c) (d)

Fig. 9 Different drift ratio belong to S453508, (a) % 0 None loading, (b) %0.6 yield stage (c) %2.7 spalling cover concrete (d) %3.4 flexural failure mode

Fig. 8 Various damage photos for S452008

Fig. 10 Various damage photos for S453508

S452008

The specimen S451008 with an axial load ratio 20% was able to reach a maximum drift of 3.4% (40 mm) before collapse. The specimen S451008 was subjected to displacement amplitudes increasing after every three cycles as a function of lateral drift. The displacement amplitudes used in the testing consisted of 0.17%, 0.34%, 0.68%, 1.0%, 1.3%, 2.0%, 2.7% and 3.4% drift until failure. Cracking and yielding occurred in third cycles. Yielding was occurred at 8 mm lateral displacement, when the lateral load reached approximately 74 kN. Spalling of the concrete cover was observed at cycle 43 at a drift of approximately 2.7%. Bar buckling and crushing at confined concrete was evident by the end of cycle 52 at a drift ratio of 3.4%. At cycle 61, the test specimen was considered to be failed. Testing was finished after the load value reached zero. The total length of the crushed concrete was about 500 mm near the footing surface, implying formation of a plastic hinge near the footing. No damage was observed above a height of 670 mm. From the ductility standpoint, assuming the first yield of the longitudinal steel as the yield point, corresponding to a drift ratio of 0.68%, the column achieved a ductility of slightly more than 5 before the flexural failure. Fig. 7 shows different stages during the second test. The damage at collapse in the vicinity of the support is shown in Fig. 8.

S453508

The amplitude of the first step of loading cycles was approximately $0.25\Delta_y$. In the first step, with a drift ratio of 0.01%, no visible cracks formed near the footing. At a drift ratio of 0.42% (5 mm deflection), first cracks were observed above the footing surface and initial yielding was measured by strain-gages. As the displacement reached a drift ratio of 1.2% (15 mm), slight crushing was observed due to spalling of the cover concrete within a height of 350 mm above the footing. At a drift ratio of 1.7% (20 mm), the steel rebar on the push and pull side buckled. The total length of the crushed concrete was about 350 mm near the footing surface, implying formation of a plastic hinge near the footing. No damage was observed above a height of 500 mm. From the ductility standpoint, assuming the first yield of the longitudinal steel as the yield point, corresponding to a drift ratio of 0.3%, the column achieved a ductility of slightly more than 4 before the flexural failure. Figure 9 shows different stages during the third test. The damage at collapse in the vicinity of the support is shown in Figure 10.

3.2 Load-displacement responses

There are many parameters that affect the behavior of RC columns. The results of previous studies are summarized briefly below.

• As the shear span ratio of RC columns increased, it was observed that the length of plastic hinge and displacement capacity increased (Cansız *et al*. 2019, Berry and Eberhard 2005).

• It was found that load carrying capacity of an RC column decreased with increasing shear span-to-effective depth ratio (Cansız *et al*. 2019).

In this study, test specimens with shear span-to-effective depth ratio of 4.5 were investigated. The program Seismo-struct was used for analyzing test specimens. The relationships between experimental load-displacement curves and numerical load-displacement curves were found to be in agreement. Load-displacement curves of test specimens are given in Fig. 11. Types of damage observed

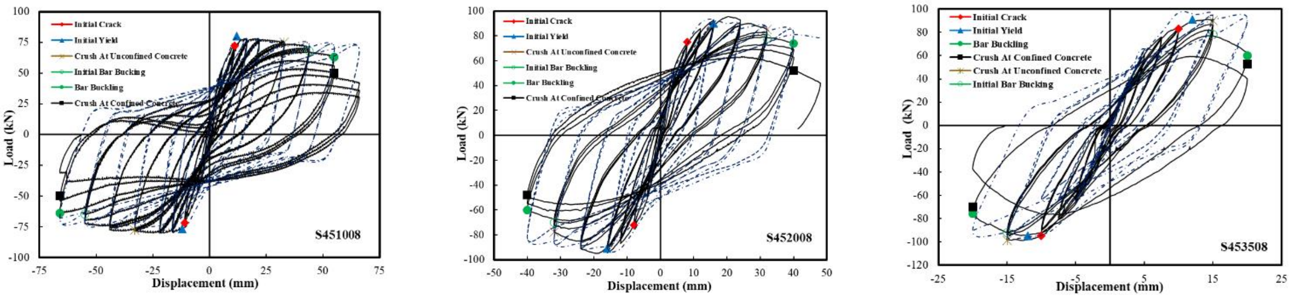

(a) (b) (c)

(———— Experimental Result, -·-·-·-·- Seismo Struct Analysis)

Fig. 11 load-displacement curves of test specimens, (a) S451008 (b) S452008 (c) S453508

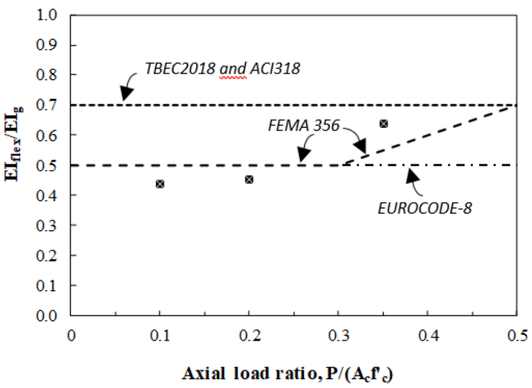

Fig. 12 Variation of reduction factor with axial load ratio for sample columns

during the experiments are marked on the load-displacement curves. All specimens reached the ultimate state with bending failure. The damage states observed in the specimens during the experiments are summarized briefly below;

- The test specimens with low axial load levels behaved more ductile than those with high axial load levels.
- When bar buckling occurred in the longitudinal reinforcement, a significant decrease in the column strength was observed.

3.3 Effective stiffness

Most seismic design codes consider stiffness of the cracked section EI_{eff} proportional to the stiffness of the gross uncracked section EI_g, specifying reduction factors to be applied to the stiffness of the uncracked cross section. EI_{eff} can be obtained from moment curvature envelope response according to Eq. (1).

$$\frac{EI_{flex}}{EI_g} = \frac{M_{0.004}}{\phi_y} \tag{1}$$

where; $M_{0.004}$ is the flexural moment at a maximum concrete compressive strain of 0.004, $\emptyset_y$ is the yield curvature and EIg is the stiffness of the gross uncracked section.

According to Turkish Building Earthquake Code (TBEC-2018), the reduction factor for the stiffness of the cracked section EI_{eff} is accepted as a constant value equal to 0.7 for RC columns. Similarly, it is accepted as 0.7 according to ACI318. EUROCODE-8 considers this value

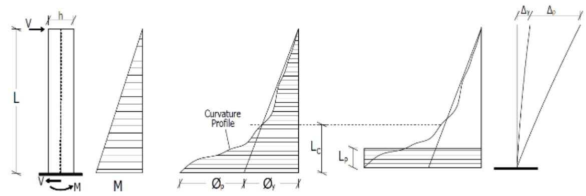

Fig. 13 Definition of plastic hinge length (Priestley and Paulay 1992)

to be 0.5. On the other hand, FEMA356 assumes a variable reduction factor depending on the axial load level. Fig. 12 presents the variation of reduction factor with axial load ratio for test specimens.

Fig. 12 shows that the stiffness of the cracked section EI_{eff} varies depending on the axial load level. FEMA356 stands out as the best representative relation to this behavior. The stiffness of the cracked section EI_{eff} with a high axial load level is more accurately estimated than that with a low axial load level in TBEC-2018 & ACI318. When the axial load level increases, it can be said that TBEC-2018 & ACI318 delivers more accurate estimates. Similarly, EUROCODE-8 estimates this value more reliably than TBEC-2018 & ACI318.

3.4 Plastic hinge length

The portion of the column over which inelastic deformations take place is commonly known as the plastic hinge; and a ductile inelastic flexural response is necessary along this region to dissipate the seismic energy. Due to uncertainty of materials and complicated interactions between constituent materials, most researchers have studied the plastic hinge of RC members by experiments. Numerous models of plastic hinge length (L_p) have been proposed by Paulay and Priestley (1992), Bae and Bayrak (2008), and Berry and Eberhard (2005).

Plastic hinges form at the maximum damage regions of RC columns. If L_p is known, the tip displacement of a column can be easily calculated by integrating curvatures. Therefore, accurate assessment of L_p is important in relating section-level response to member-level response of a concrete column. The length of a plastic hinge depends on many parameters. The parameters influencing the length of a plastic hinge are axial load level, moment gradient, shear stress level in the plastic hinge region, mechanical

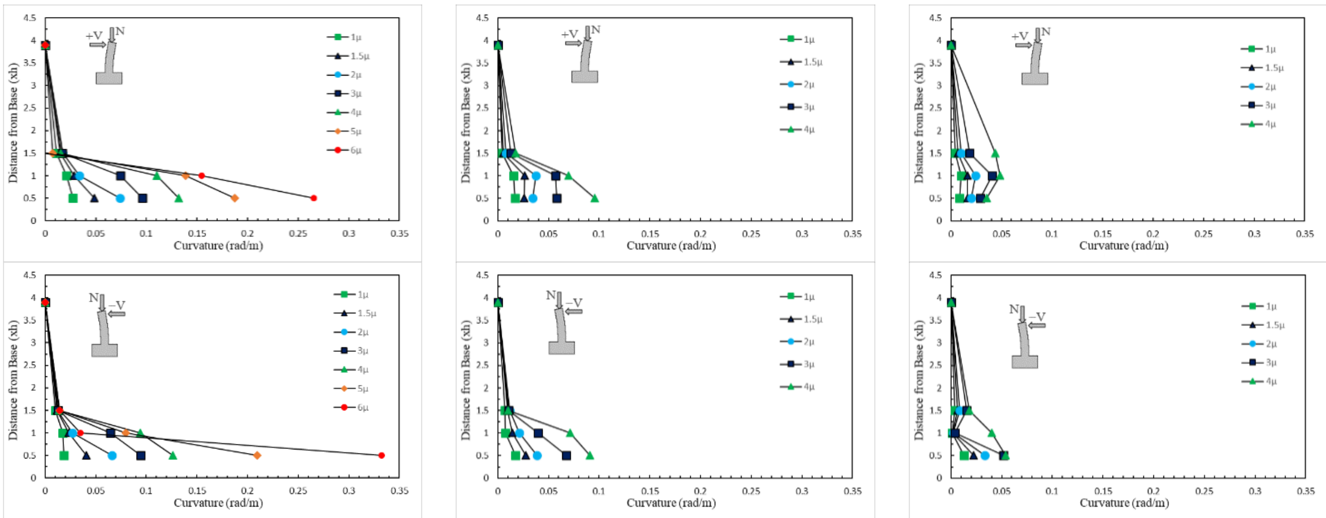

S451008 S452008 S453508

Fig. 14 Effect of axial load on curvature profiles

properties of longitudinal and transverse reinforcement, concrete strength and level of confinement and its effectiveness in the potential hinge region.

Priestley and Paulay proposed a plastic hinge model in 1992. They simplified the curvature distribution along the length of a column using a plastic hinge (Fig. 13). Using the second moment area theorem, they calculated the length of plastic hinge as

$$L_p = 0.08L + 0.022 d_b f_y \tag{2}$$

where d_b is the longitudinal reinforcement diameter, L is the column length and f_y is the yield strength of longitudinal reinforcement. The length of the plastic hinge suggested by ACI318 is given in Eq. (3).

$$L_p = 0.5h \tag{3}$$

Similarly, plastic hinge length is considered as 0.5h in TBEC-2018.

Bae and Bayrak (2008) proposed Eq. (6) for the calculation of L_p in RC columns.

$$\frac{L_p}{h} = \left[0.3\left(\frac{P}{P_o}\right) + 3\left(\frac{A_s}{A_g}\right) - 0.1\right]\frac{L}{h} + 0.25 \geq 0.25 \tag{4}$$

where; h is the height of column, P is the axial load, P_o is the nominal axial load capacity as per ACI-318, As is the area of tension reinforcement and A_g is the gross area of concrete section.

Effect of Axial Load

The curvature profiles along the length of the columns were investigated for various axial load levels. Fig. 14 shows a brief summary of the results of the analyses. As can be observed in Fig. 14, the curvature profiles effectively show the effect of axial load level. The test specimen with a low axial load level (S451008) behaved more ductile, and the curvature reached higher values. In contrast, the test specimen with a high axial load level (S453508) behaved less ductile and the curvatures reached a lower value compared to the other specimens.

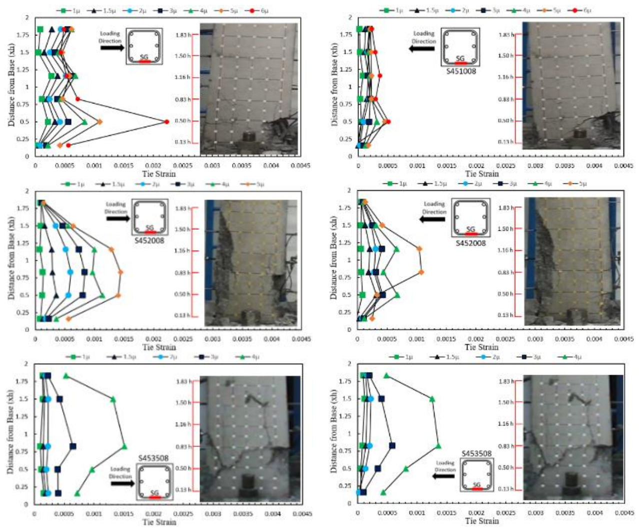

Fig. 15 Comparison of plastic hinge length for tested columns

The damage observed within the plastic hinge region of each test specimen and the corresponding tie strains along the columns are shown in Fig. 15. S451008-S452008-S453508 were subjected to constant compressive axial loads of 292.5 kN (10%), 595 kN (20%) and 1000 kN (35%), respectively. Fig. 15 shows that the severely damaged regions of S453508 and S452008 are longer than that of S451008. The tie strains measured along the columns at the failure loading cycles also illustrate that S453508 and S452008 experienced inelastic tie strains over a longer length than S451008. Many ties in S453508 and S452008 experienced inelastic strains larger than the measurement limits of strain gages at the failure loading cycle. Therefore, it can be concluded that, for the specimens tested in this study, L_p increased as the level of axial load increased.

For low axial load levels (0.1 $N/A_c f_c$), L_p is approximately 0.75h. Reaching at an axial load of approximately 0.2 $N/A_c f_c$, the L_p increases with increasing

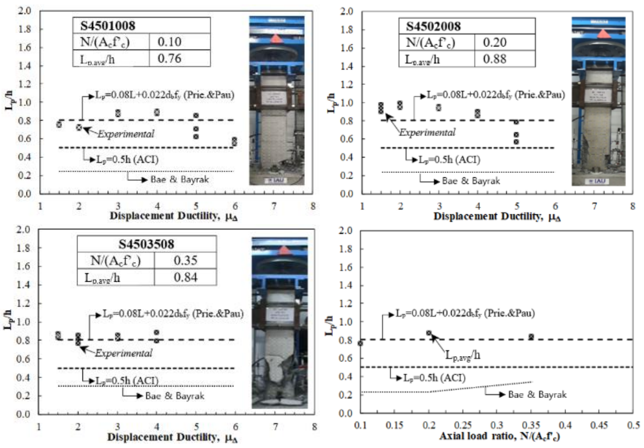

Fig. 16 Comparison of plastic hinge length for tested columns

axial load. At a moderate axial load level, L_p is 0.90h. For a high axial load level (0.35 N/A_cf_c), L_p is approximately 0.80h. Priestley and Paulay's proposal suitably estimates the length of the plastic hinge. However, it is known that the plastic hinge region changes depending on the axial load according to strain values obtained from the lateral reinforcement. The proposal of Priestley and Paulay does not take into account the effect of the axial load. Therefore, the Priestley and Paulay suggestion may not give proper results for columns with higher axial load levels. Figure 16 illustrates comparison of plastic hinge length for tested columns.

4. Displacement capacity of RC column

The displacement capacity of RC elements has been investigated by many researchers in recent years. Some of the studies in this area are considered as limit values in the codes. In this study, codes and analytical methods were used for estimating the displacement capacity of RC members.

4.1 Displacement capacity in codes

Within the scope of this study, Turkey Building Earthquake Code (2018), EUROCODE-8 and FEMA356 regulations were examined.

Turkey Building Earthquake Code (TBEC-2018)

In the nonlinear static procedure of TBEC-2018, in order to predict the performance level, the strain limits of concrete and steel are used as the main parameters. Moreover, Turkey Building Earthquake Code (2018) defines three damage levels based on the ductility capacity and predicts failure mode. Seismic performance of a structure can be determined by considering the distribution of structural damage along the building. For a RC column, sectional damage state should be calculated by determining the strain values of concrete fibers and reinforcement. Strain limits for collapse limits are provided as

$$\varepsilon_c^{CP} = 0.0035 + 0.07\sqrt{\omega_{wc}} \leq 0.01 \tag{5}$$

$$\varepsilon_s = 0.4\varepsilon_{su} \tag{6}$$

$$\theta_p = \frac{2}{3}\left[(\emptyset_u - \emptyset_y)L_p\left(1 - 0.5\frac{L_p}{L_s}\right) + 4.5\emptyset_u d_b\right] \tag{7}$$

where, ε_c is the core concrete strain at the outer fiber of the confined region, ε_s is the steel strain at the critical section, ε_{su} is the steel strain at the maximum strength, w_{we} is the mechanical transverse reinforcement ratio, $\emptyset_u$ is the maximum curvature of section, $\emptyset_y$ is the yield curvature of section, L_p is the plastic hinge length, L_s is the shear span and d_b is the longitudinal bar diameter.

EUROCODE-8

EUROCODE-8 includes a part for the assessment of RC columns that proposes the calculation of chord rotations with the given equations in the code. These equations are functions of many variables such as axial load ratio, longitudinal reinforcement ratio, transverse reinforcement ratio and yield strength of the transverse reinforcement. In EUROCODE-8, three limit states that correspond to the previously mentioned performance levels are employed; Damage Limitation (DL), Significant Damage (SD) and Near Collapse (NC). A corresponding chord rotation value is given for each limit state. The total chord rotation capacity for the limit state of NC (sum of elastic and plastic behavior) should be calculated from the following expression

$$\theta_{um} = \frac{1}{\gamma_{el}} 0.016x0.3^{\vartheta}\left(\frac{\max(0.01w')}{\max(0.01w\ \ )} f_c\right)^{0.225} \left(\min\left(9;\frac{L_v}{h}\right)\right)^{0.35} 25^{\left(\alpha\rho_{sx}\frac{f_{yw}}{f_c}\right)}(1.25^{100\rho_d}) \tag{8}$$

where, γ_{el} is the seismic element coefficient (equal to primary element is 1.5, secondary element is 1), ϑ is the dimensionless axial load level (N/A_cf_c), h is the height of section, w is the mechanical reinforcement ratio for compression and tension, L_v is the shear span, f_c is the concrete strength, f_{yw} is the transverse steel yield strength, ρ_{sx} is the ratio of transverse steel to parallel to the direction x of loading, α is the confinement effectiveness factor, ρ_d is the steel ratio of diagonal reinforcement. Similarly, the EUROCODE-8 regulation provides the plastic rotation capacity as

$$\theta_{um}^{pl} = \frac{1}{\gamma_{el}} 0.0145x0.25^{\vartheta}\left(\frac{\max(0.01w')}{\max(0.01w\ \ )}\right)^{0.3} (f_c)^{0.2} \left(\min\left(9;\frac{L_v}{h}\right)\right)^{0.35} 25^{\left(\alpha\rho_{sx}\frac{f_{yw}}{f_c}\right)}(1.25^{100\rho_d}) \tag{9}$$

where, γ_{el} is equal to 1.8.

FEMA356

FEMA 356 is the American pre-standard and commentary for the seismic rehabilitation of buildings. The document expresses deformation limits, which are in the form of plastic rotations. In FEMA 356, deformation limits are specified in terms of plastic rotation for RC columns.

Table 4 Drift ratio for collapse limits state in codes

Code	$\theta_{plastic}$			θ_{total}		
	Specimen Name			Specimen Name		
	S451008	S452008	S453508	S451008	S452008	S453508
TBEC-2018	0.025	0.014	0.010	0.030	0.020	0.017
EUROCODE-8	0.024	0.021	0.017	0.035	0.031	0.026
FEMA356	0.020	0.018	0.016	0.025	0.024	0.023

These limit values are directly related with the failure mode of behavior (shear or flexure), $N/(A_g f_c)$ ratio (axial load ratio), the spacing of stirrups, and $(V/(b_w d\sqrt{f_c})$ ratio. The plastic capacity for the limit state of Collapse Prevented (sum of elastic and plastic behavior) should be calculated from the following expression

$$\frac{P}{A_g f_c} \leq 0.1 \rightarrow \frac{V}{b_w d\sqrt{f}_c} \leq 3 \rightarrow \theta_{pl} = 0.020 \quad (10)$$

$$\frac{P}{A_g f_c} \leq 0.1 \rightarrow \frac{V}{b_w d\sqrt{f}_c} \geq 6 \rightarrow \theta_{pl} = 0.016 \quad (11)$$

$$\frac{P}{A_g f_c} \geq 0.4 \rightarrow \frac{V}{b_w d\sqrt{f}_c} \leq 3 \rightarrow \theta_{pl} = 0.015 \quad (12)$$

$$\frac{P}{A_g f_c} \geq 0.1 \rightarrow \frac{V}{b_w d\sqrt{f}_c} \geq 6 \rightarrow \theta_{pl} = 0.012 \quad (13)$$

where, P is the axial load, A_g is the area of section, f_c is the concrete strength, V is the maximum shear force, b_w is the width of section and d is the height of effectiveness.

4.2 Comparison with codes and analytical method

According to TBEC-2018, FEMA 356 and EUROCODE-8, performance limits for each performance level were determined. These values are shown in Table 4 and Table 5. Park and Paulay (1975) calculated the tip displacement of a column as

$$\Delta_{total} = \Delta_y + \Delta_p = \frac{\emptyset_y L^2}{3} + (\emptyset_u - \emptyset_y) l_p (L - L_p) \quad (14)$$

$$\Delta_{total} = \Delta_y + \theta_p (L - L_p) \quad (15)$$

The plastic rotations given in Table 4 were converted to displacements by Eq. (15).

Flexure critical columns selected for parametric study were analyzed and the capacity curves were obtained. Performance limits for each performance level were calculated according to TBEC-2018, FEMA 356 and EUROCODE-8.

Performance limits corresponding to each performance level obtained by different seismic guidelines were compared. Fig. 17 illustrate load-displacement curves with ultimate damage limits obtained according to different seismic guidelines. For the performance level of collapse prevention, total drift ratios for TBEC-2018, EUROCODE-8 and FEMA356 are 3.00%, 3.50% and 2.50%, respectively for S451008. For the performance level of collapse prevention, total drift ratios of TBEC-2018, EUROCODE-8 and FEMA356 are 2.00%, 3.10% and 2.40%, respectively for S452008. For the performance level of collapse prevention, total drift ratios for TBEC-2018, EUROCODE-8 and FEMA356 are 1.70%, 2.60% and 2.30%, respectively

Table 5 Lateral displacement capacity and relative error for test specimens

Specimen Name	Code			Experiment
	$\Delta_{tot.}$ (mm)/(% Relative Error)			Δ_{um} (mm)
	TBEC-2018	EUROCODE-8	FEMA356	$\Delta_{V=0.8\,Vmax}$
S451008	34.54 (%29)	30.41 (%37)	26.33 (%45)	48.70
S452008	23.50 (%21)	29.17 (%2)	26.11 (%12)	29.80
S453508	16.70 (%6)	25.55 (%62)	24.53 (%56)	15.70

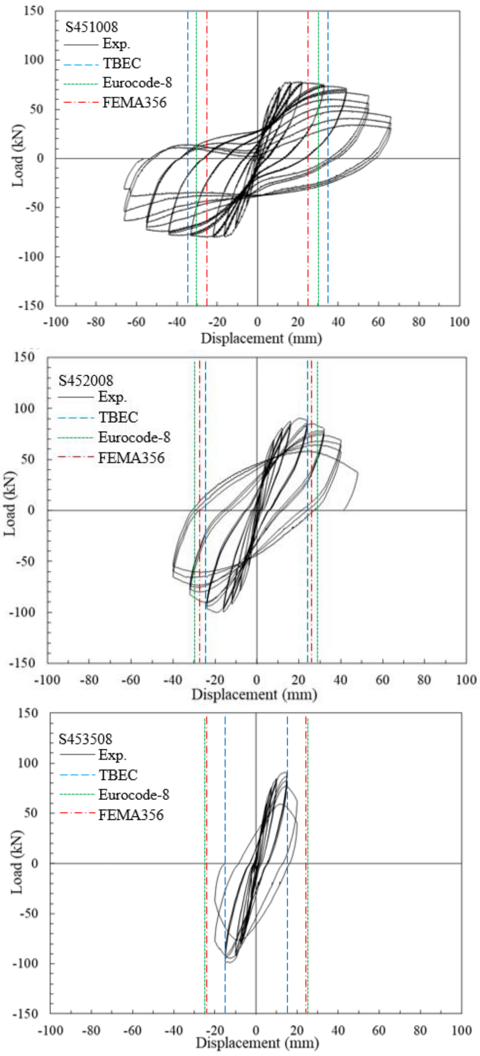

Fig. 17 Load-displacement curves of test specimens and ultimate damage limits for codes

for S453508. The plastic rotation capacity of a RC column according to TBEC-2018 depends on properties of materials, curvature of section, shear span and plastic hinge length. EUROCODE-8 calculates the plastic rotation capacity of a RC column based on properties of materials, height of section, dimensionless axial load level, confinement factor and seismic element coefficient. FEMA356 determines the plastic rotation capacity of a RC column depending on less parameters. These parameters are dimensionless axial load level, base shear force and properties of materials. As this situation is examined, it was observed that EUROCODE-8 considers more parameters than the other codes. When standard deviations are compared, it was observed that TBEC-2018 provided closer estimates and smaller relative error values for all performance levels compared to the other seismic codes. For TBEC-2018, sectional damage state was calculated by determining the strain values of concrete fibers and reinforcement. Experimental results show that TBEC-2018 delivers the most accurate estimates than the other seismic codes for the considered axial load levels.

5. Conclusions

Based on the experimental results and comparisons with the estimates of codes, the conclusions drawn is summarized below.

• TBEC-2018 delivered closer estimates and smaller relative error values for all performance levels compared to other seismic codes. This may result from the fact that TBEC-2018 takes into account material strain values as limit values for assessing performance level of RC columns.

• EUROCODE-8 and FEMA 356 can give improper results at high axial load levels for the collapse limit state. While calculating the drift capacity, the effect of the axial load should be considered more in EUROCODE-8 and FEMA356.

• The length of the plastic hinge region increased with axial load. The strain diagram of the lateral reinforcement clearly showed this situation. This is also supported by the damage observed at failure. Damage at the low axial load (10%) level was concentrated below the second stirrup ($\sim 0.5h$). However, damage was observed at the levels of third and fourth stirrups ($\sim 1.2h$) for high axial load levels (35%).

• The proposal of Paulay and Priestley (1992) correctly determines the length of the plastic hinge without axial load effect. However, plastic hinge length is affected by axial load level. ACI318 and TBEC consider the length of the plastic hinge as constant 0.5h. Although Bae and Bayrak's proposal has taken into consideration the effect of axial load on the length of the plastic hinge, it may not give improper results.

The behaviour of the whole structure is not necessarily the same as the behaviour of an individual column. This study focuses on the behaviour of columns individually, so it neglects the effect of other frame elements.

Acknowledgments

This work was supported by Research Fund of the Yildiz Technical University (Project Number: 2016-05-01-DOP02) and Department of Scientific Research Project of Istanbul Aydin University (Project Number: BAP-2017-01).

References

Abadi, H., Paton-Cole, V., Patel, V. and Thai, H. (2019), "Axial strength and elastic stiffness behaviour of partially confined concrete columns", *Constr. Build. Mater.*, **196**, 727-741.

Abdullah, S. and Wallace, J. (2019), "Drift capacity of RC structural walls with special boundary elements", *ACI Struct. J.*, **116**(1), 183.

ACI 318 (2011), Building Code Requirements for Structural Concrete and Commentary, American Concrete Institute, Farmington Hills, MI, USA.

Arslan, G., Hacısalihoğlu, M., Balci, M. and Borekci, M. (2013), "An investigation on seismic design indicators of RC columns using finite element analyses", *Int. J. Civil Eng.*, **12**(2), 237-243.

Aschheim, M. (2002), "Seismic design based on the yield displacement", *Earthq. Spectra*, **18**(4), 581-600.

Au, F. and Bai, Z. (2006), "Effect of axial load on flexural behaviour of cyclically loaded RC columns", *Comput. Concrete*, **3**(4), 261-284.

Bae, S., Mieses, A. and Bayrak, O. (2005), "Inelastic buckling of reinforcing bars", *J. Struct. Eng.*, **131**(2), 314-321.

Bae, S. and Bayrak, O. (2008), "Plastic hinge length of reinforced concrete columns", *ACI Struct. J.*, **105**(3), 290-300.

Behnam, B. and Shojaei, F. (2018), "A risk index for mitigating earthquake damage in urban structures", *Integrating Disaster Science and Management*, Elsevier.

Berry, M. and Eberhard, M. (2005), "Practical performance model for bar buckling", *J. Struct. Eng.*, **131**(7), 1060-1070.

Bhosale, A., Davis, R. and Sarkar, P. (2017), "Vertical irregularity of buildings: Regularity index versus seismic risk", *ASCE-ASME J. Risk Uncert. Eng. Syst. Part A: Civil Eng.*, **3**(3), 04017001.

Brachmann, I., Browning, J. and Matamoros, A. (2004), "Drift dependent confinement requirements for reinforced concrete columns under cyclic loading", *ACI Struct. J.*, **5**(101), 669-677.

Cao, V., Ronagh, H. and Baji, H. (2014), "Seismic risk assessment of deficient reinforced concrete frames in near-fault regions", *Adv. Concrete Constr.*, **2**(4), 261-280.

Cansız, S., Aydemir, C. and Arslan, G. (2019), "A new damage index model dependent displacement ductility for reinforced concrete columns", *Struct. Eng. Mech.* (under Review).

Cansız, S., Aydemir, C. and Arslan, G. (2019), "A new damage index for reinforced concrete columns", *Earthq. Struct*. (under Review).

Cao, V. and Ronagh, H. (2013), "A model for damage analysis of concrete", *Adv. Concrete Constr.*, **1**(2), 187-200.

CEN (2003), Eurocode 8: Design of Structures for Earthquake Resistance-Part 3, Comité Européen de Normalisation, Brussels.

Elwood, K. and Moehle, J. (2005), "Drift capacity of reinforced concrete columns with light transverse reinforcement", *Earthq. Spectra*, **21**(1), 71-89.

FEMA-356 (2000), "Prestandard and commentary for the seismic rehabilitation of buildings", Report No. FEMA-356, Federal Emergency Management Agency, Washington, D.C.

Gharehbaghi, S., Moustafa, A. and Salajegheh, E. (2016), "Optimum seismic design of reinforced concrete frame structures", *Comput. Concrete*, **17**(6), 761-786.

Kang, J. and Lee, J. (2016), "A new damage index for seismic fragility analysis of reinforced concrete columns", *Struct. Eng. Mech.*, **60**(5), 875-890.

Lehman, D.E. and Moehle, J.P. (2000), "Seismic performance of well-confined concrete bridge columns", PEER-1998/01. Pacific Earthquake Engineering Research Center, University of California, Berkeley.

Mander, J.B., Priestley, M.J.N. and Park, R. (1988), "Theoretical stress-strain model for confined concrete", *J. Struct. Eng.*, ASCE, **114**(8), 1804-1826.

Nishitani, A., Matsui, C., Hara, Y., Xiang, P., Nitta, Y., Hatada, T., Katamura, R., Matsuya, I. and Tanii, T. (2015), "Drift displacement data based estimation of cumulative plastic

deformation ratios for buildings", *Smart Struct. Syst.*, **15**(3), 881-896.
NZSEE (2017), The Seismic Assessment of Existing Buildings. Technical Guidelines for Engineering Assessments. Part C - Detailed Seismic Assessment. Section C5 - Concrete Buildings, New Zealand Society for Earthquake Engineering.
Panagiotakos, T.B. and Fardis, M.N. (2001), "Deformation of reinforced concrete members at yielding and ultimate", *ACI Struct. J.*, **98**(2), 135-148.
Park, R. and Paulay, T. (1975), *Reinforced Concrete Structures*, John Wiley and Sons, New York.
Paulay, T. and Priestley, M.J.N. (1992), *Seismic Design of Reinforced Concrete and Masonry Buildings*, John Wiley and Sons, New York.
Priestley, M.J.N. and Park, R. (1987), "Strength and ductility of concrete bridge columns under seismic loading", *ACI Struct. J.*, **84**(1), 61-76.
Priestley, MJN. and Kowalsky, MJ. (1998), "Aspects of drift and ductility capacity of cantilever structural walls", *Bull. NZ Nat. Soc. Earthq. Eng.*, **2**(31), 73-85.
Priestley, M.J.N., Calvi, G.M. and Kowalsky, M.J. (2007), *Displacement-Based Seismic Design of Structures*, IUSS Press, Foundazione EUCENTRE, Pavia.
Pujol, S., Sozen, M.A. and Ramirez, J.A. (2006), "Displacement history effects on drift capacity of reinforced concrete columns", *ACI Struct. J.*, **103**(2), 253-262.
Puranam, A., Wang, Y. and Pujol, S. (2018), "Estimating drift capacity of reinforced concrete structural walls", *ACI Struct. J.*, **115**(6), 1563-1574.
Sezen, H. (2008), "Shear deformation model for reinforced concrete columns", *Struct. Eng. Mech.*, **28**(1), 39-52.
Shojaei, F. and Behnam, B. (2017), "Seismic vulnerability assessment of low-rise irregular reinforced concrete structures using cumulative damage index", *Adv. Concrete Constr.*, **5**(4), 407-422.
TBEC (2018), Turkey Building Earthquake Code, Specifications for Structures to be Built in Disaster Areas, Ankara.
Wibowo, A., Wilson, J., Lam, N. and Gad, E. (2014), "Drift capacity of lightly reinforced concrete columns", *Aust. J. Struct. Eng.*, **15**(2), 131-150.
Zhou, X., Tu, X., Chen, A. and Wang, Y. (2019), "Numerical simulation approach for structural capacity of corroded reinforced concrete bridge", *Adv. Concrete Constr.*, **7**(1), 11-22.

CC